# Peculiarities of internal vibrational modes of $Cs_2CdBr_4$ crystal

Shchur Ya.I., Trach I.B., Vlokh O.G.

Institute of Physical Optics, Dragomanova 23, Lviv, 79005, Ukraine

Received 12.11.2001

## Abstract

Lattice dynamics study of $Cs_2CdBr_4$ crystal comprising both the Raman-scattering experiment and numerical simulation has been performed in the high-temperature orthorhombic phase (Pnma). The observation of extra Raman lines, forbidden by factor-group analysis reveals an existence of orientational disorder of the $CdBr_4^{2-}$ groups. An interpretation of Raman spectra was made in the framework of a semi-empirical model taking into consideration the long-range Coulumbic, short-range and covalent interactions. The agreement between the theoretical and experimental phonon frequencies is reasonable.

**Key words:** lattice dynamics, phonon, Raman spectra

**PACS:** 63.20.Dj

## Introduction

The $Cs_2CdBr_4$ crystal belongs to the well known $A_2BX_4$ type compounds with $\beta$-$K_2SO_4$ structure at room temperature (Pnma space group, Z=4 [1]). Plesko et al. [2,3] reported results of NQR and X-ray measurements indicating that at $T_1$=252K crystal undergoes a transition from the normal to the incommensurate phase, modulated in the x-direction with $\mathbf{k}_0 \approx 0.15\mathbf{a}$. The physical properties of this crystal were widely studied by X-ray diffraction [4-6], dielectric measurements [4], acoustic and optical investigations [7]. Lattice dynamics was studied by means of Brillouin scattering [8,9], Raman scattering method [10,11] and infrared spectroscopy [12,13]. However, an explanation of some peculiarities of lattice dynamics, especially a correct interpretation of the internal vibrations, has been still missing.

In this report we present results of lattice-dynamical investigation of the high-frequency spectral region corresponding to the internal stretching vibrations of the $CdBr_4^{2-}$ groups. This type of vibration is very sensitive to the any minor changes of crystal structure like crystal imperfections or an appearance of modulated structure. The careful line-shape fitting of stretching modes was combined with the numerical simulation of vibrational spectrum at Brillouin zone centre.

## Experimental

Single crystals of $Cs_2CdBr_4$ were grown by the Bridgman method from the melt of CsBr and $CdBr_2$ in a molar ratio of 2:1 [14]. CsBr and $CdBr_2 \cdot 4H_2O$ were dried at 220°C in the air, mixed carefully and then dried in a quartz ampoule at 260°C under vacuum. The ampoule was then sealed and used for Bridgman growth

at a rate of 0.5 mm $h^{-1}$. The sample was prepared from optically homogeneous parts by cutting with a diamond saw, grinding and polishing with diamond pastes. The specimen had a shape of parallelepiped with the size 7×7×6 $mm^3$. The crystallographic axes were determined by the X-ray method.

Raman spectra were excited with polarized radiation of an LGN-402 argon ion laser ($\lambda_0$=488 nm; approximate power, 180 mW) and recorder with a DFS-52 spectrometer in the 90° scattering configuration. The spectra width of the slits was 2 $cm^{-1}$.

## Results and discussion

According to the group theory analysis in a high-temperature phase the 84 vibrational modes of $Cs_2CdBr_4$ crystal in the Brillouin zone centre (**k**=0) can be classified as follows:

$$G = 13A_g + 8B_{1g} + 13B_{2g} + 8B_{3g} + 8A_u + 13B_{1u} + 8B_{2u} + 13B_{3u}, \quad (1)$$

All modes with gerade symmetry concerning a centre of inverse ($A_g$, $B_{1g}$, $B_{2g}$ and $B_{3g}$) are Raman active. The Raman spectra of $Cs_2CdBr_4$ crystal measured for various scattering geometries at room temperature are shown in Fig. 1. Due to the large mass of the atoms of $Cs_2CdBr_4$ crystal the Raman active frequencies do not exceed 200 $cm^{-1}$. The spectra were fitted by a sum of damped oscillators. It turns out that we can fit the experimental data using a lesser number of modes than it was predicted by group theory. The values of all frequencies are presented in Table 1.

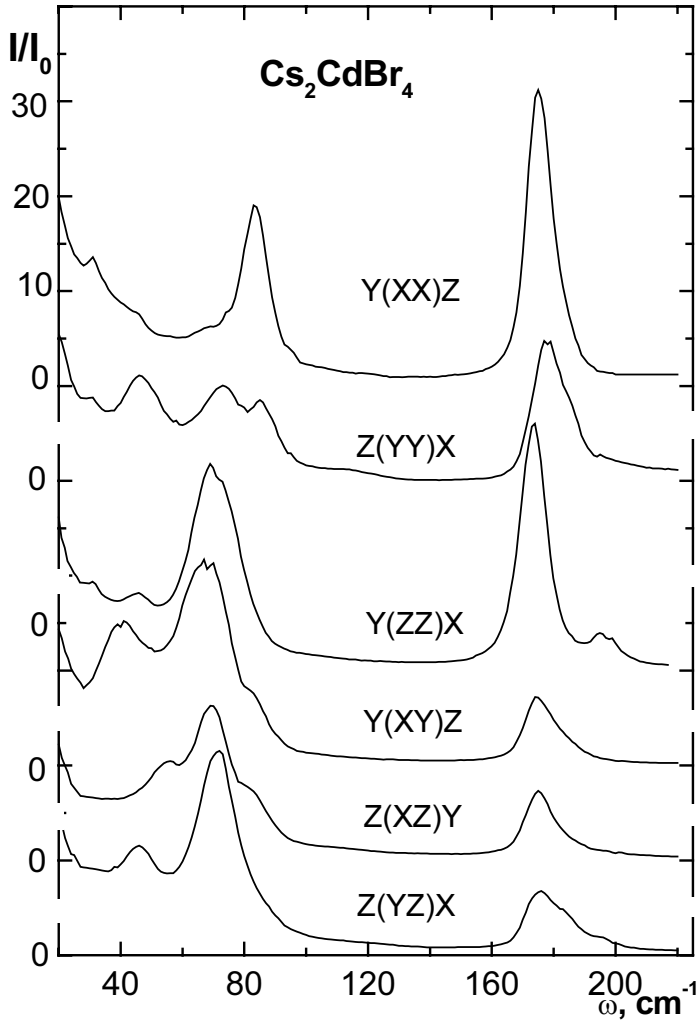


**Fig. 1.** Raman spectra of $Cs_2CdBr_4$ at room temperature (Pnma phase).

Table 1. Comparison of the calculated and experimental values of phonon frequencies ($cm^{-1}$) at the centre of the Brillouin zone in Pnma phase.

| $A_g$ | | $B_{1g}$ | | $B_{2g}$ | | $B_{3g}$ | |
|---|---|---|---|---|---|---|---|
| Calcul. | Raman | Calcul. | Raman | calcul. | Raman | calcul. | Raman |
| 23 | | 23 | | 26 | | 23 | 22 |
| 27 | 28 | 28 | | 30 | | 33 | |
| 31 | | 46 | 39 | 33 | | 40 | 43 |
| 36 | | 68 | 66 | 50 | | 64 | |
| 44 | 43 | 70 | 79 | 54 | 52 | 68 | 68 |
| 54 | 66 | 105 | 171 | 57 | 65 | $\nu_1$107 | 172 |
| 69 | 70 | 145 | 175 | 73 | 74 | $\nu_3$146 | 175 |
| 93 | 81 | $\nu_3$181 | 182 | 93 | 79 | $\nu_3$181 | 178 |
| 135 | | | | 137 | | | |
| 143 | | | | 146 | | | |
| $\nu_1$175 | 173 | | | $\nu_1$177 | 172 | | |
| $\nu_3$187 | | | | $\nu_3$188 | 177 | | |
| $\nu_3$206 | 194 | | | $\nu_3$206 | | | |

The free $CdBr_4^{2-}$ ion is tetrahedral and thus has four distinct vibrational frequencies (a nondegenerate $A_1$ mode, a doubly degenerate E-mode, and two triply degenerate modes of $F_2$ type). The correlation diagram of internal vibrations is presented in Table 2. These modes belong to the two spectral regions. According to the references [15] stretching modes lie in the ranges 161-166 $cm^{-1}$ ($\nu_1$) and 177-181 $cm^{-1}$ ($\nu_3$) whereas the bending vibrations are located near 49-53 $cm^{-1}$ ($\nu_2$) and 61-75 $cm^{-1}$ ($\nu_4$). It is obvious that bending modes fall in the region of external lattice vibrations. Perhaps, this is the main peculiarity of $Cs_2CdBr_4$ lattice dynamics, which seriously hinders its analysis.

As seen from Table 2 the group-theory predicts the three high-frequency stretching vibrations ($\nu_1$, $2\nu_3$) in the $A_g$ and $B_{2g}$ Raman spectra and only one ($\nu_3$) stretching mode can be active in the $B_{1g}$ and $B_{3g}$ spectra. However

Table 2. Correlation diagram of the internal modes in the high-temperature (*Pnma*) phase.

| Free ion $(CdBr_4)^{2-}$ symmetry | Site symmetry | Factor-group symmetry |
|---|---|---|
| $T_d$ | $C_{1h}$ | $C_{2h}$ |

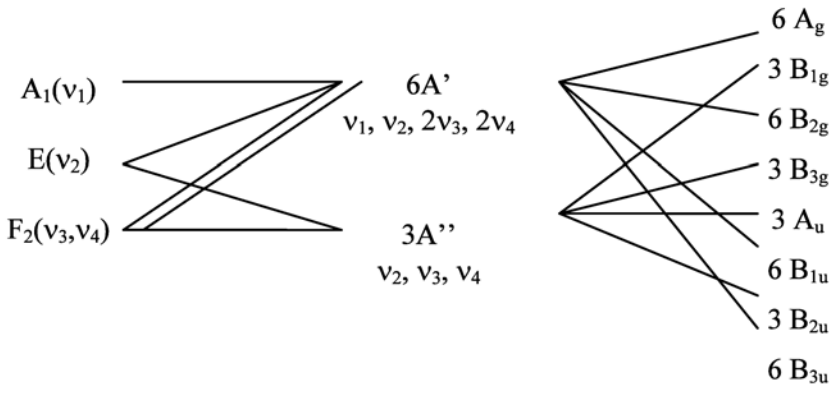

instead of one "allowed" line of $B_{1g}$ and $B_{3g}$ symmetry other lines appear in this region. In order to fit correctly the high-frequency part of $B_{1g}$ and $B_{3g}$ spectra, we were forced to introduce three damped oscillators for each symmetry (see Table 1). Fig. 2,3 present Raman spectra in the stretching mode region together with deconvoluted individual modes.

The explanation may be suggested as follows. The correlation diagram of internal vibrations (Table 2) is valid only for strict *Pnma* symmetry. Such a structure was determined by X-ray experiment [16] which can detect only a "static" space-averaged crystal structure. Within the *Pnma* symmetry the $CdBr_4^{2-}$tetrahedron has $C_{1h}$ local symmetry, that is it must obey strictly to the mirror symmetry. However as it was shown by Itoh [17] for $Rb_2ZnCl_4$ crystal possessing a similar structure, the $ZnCl_4^{2-}$ clusters occupy with equal probability positions around the mirror plane. In other words, the instantaneous structure of $Rb_2ZnCl_4$ and perhaps of the other compounds of this type is noncentrosymmetric. Contrary to X-ray diffraction the Raman scattering occurs in a very short time, much shorter then the one needed for a jump between two quasi-equilibrium positions. In this sense the Raman scattering brings a additional information about the peculiarities a crystal structure.

The main consequence of this phenomenon is a violation of selection rule validity. Thus, it can evoke the lowering of tetrahedron local symmetry to $C_1$ . It means the all nine internal vibrations should be visible in all geometries of Raman scattering. In other words the mixing of the gerade and ungerade type of modes can happen. Consequently, the three vibrations ($\nu_1$, $2\nu_3$) are expectable in the stretching mode spectral region. Exactly such a number of modes was detectable by us in the high-frequency region of $B_{1g}$(XY) and $B_{3g}$.(YZ) spectra (see Fig. 2,3 and Table1).

It is worthwhile noticing that the extra lines in the internal vibration range have been previously determined in the normal phase of $K_2SeO_4$ [18] and $Rb_2ZnCl_4$ [19] crystals. We would like to mention the conclusions of the work of de Pater [n] supporting indirectly the results presented in our report. It was found that the regions of incommensurate order are randomly distributed in the normal phase of $Rb_2ZnBr_4$ crystal.

## Model and group-theory classification

In order to interpret our Raman data we have

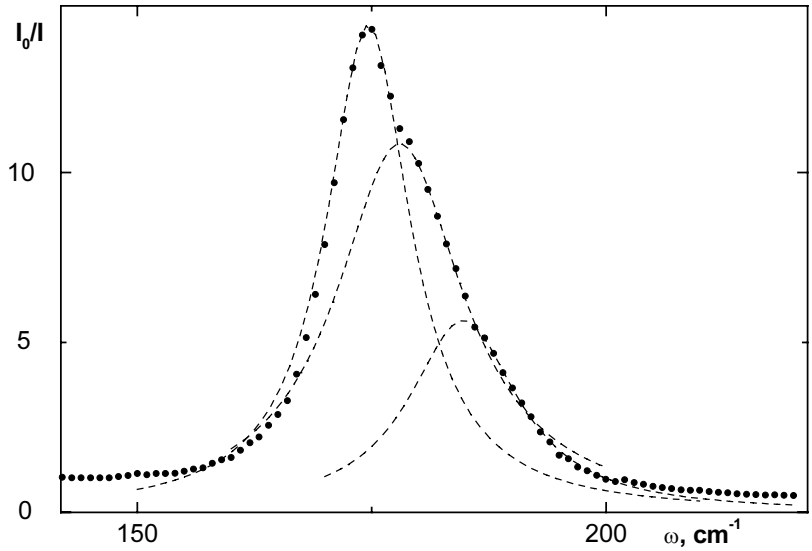


**Fig. 2.** High-frequency region of $B_{1g}$(XY) spectra

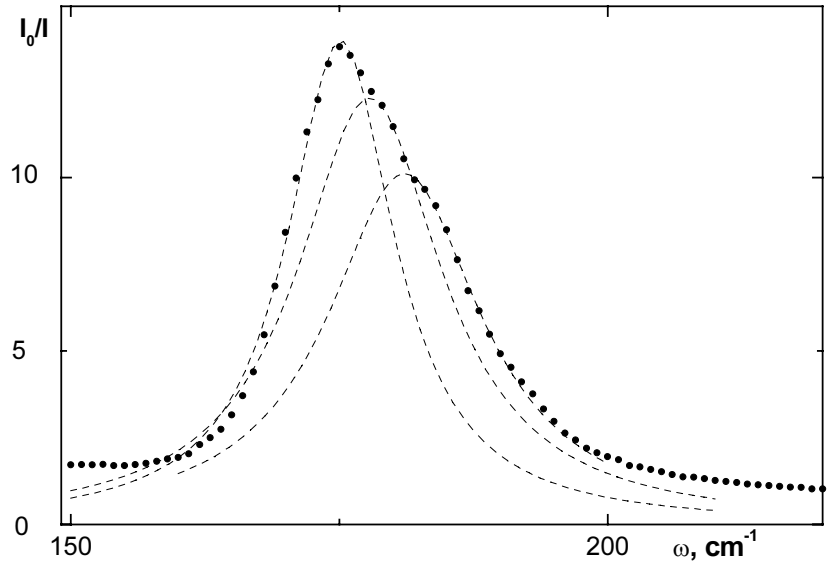


**Fig. 3.** High-frequency region of $B_{3g}$.(YZ) spectra

carried out a numerical simulation of lattice dynamics. The lattice modeling of the $Cs_2CdBr_4$ crystal was performed in the framework of the atomistic model [20] taking into consideration both the external and the internal vibrations. However, Cs, Cd and Br atoms in $Cs_2CdBr_4$ are connected by different types of interactions. For simulation of ionic interactions between Cd and Br atoms, which belong to the different $CdBr_4^{2-}$ groups and Cs atoms, we have used the two-body interatomic potential in the following form [20]:

$$V(r_{kk'}) = \frac{e^2}{4\pi\varepsilon_0}\frac{Z(k)Z(k')}{r_{kk'}} + aexp\left(-\frac{br_{kk'}}{R(k)+R(k')}\right), \quad (2)$$

where the first term corresponds to the long-range Coulombic interactions and the second one describes the short-range repulsive interaction of the Born-Mayer type. $Z(k)$ and $R(k)$ are the effective charge and radius of atom $k$, respectively; $r_{kk'}$ is the distance between the atoms of k and k' kind; a and b constants have the values a=1822eV and b=12.364 [21].

To approximate the covalent stretching interactions within the Cd-Br bond we used, in accordance with [20], the following expression:

$$V(r_{CdBr}) = -D\exp\left(-\frac{n}{2}\frac{(r_{CdBr}-r_0)^2}{r_{CdBr}}\right), \quad (3)$$

where $r_{CdBr}$ is the distance between the covalent linked Cd and Br atoms; $n$, $D$ and $r_0$ are treated as parameters.

For the simulation of bending vibrations which are due to the Br-Br interactions within the same $CaBr_4^{2-}$ groups the following potential [20] was used:

$$V(r_{BrBr}) = \frac{e^2}{4\pi\varepsilon_0}\frac{Z^2(Br)}{r_{BrBr}} + Saexp\left(-\frac{br_{BrBr}}{2R(Br)}\right) - \frac{W}{r_{BrBr}^6}, \quad (4)$$

where S and W are parameters. The first and second terms in (4) have the meanings similar to those used in expression (2) and the third one is the potential van der Waals type.

The unknown parameters in the expression (2) were determined from the lattice equilibrium conditions and also with respect to the electrical neutrality condition ($\sum_k z(k) = 0$).

The parameters of bond-stretching (3) and Br-Cd-Br angle-bending (4) potentials were obtained from the condition of the best agreement between the calculated and

experimental frequencies of IR- and Raman-active modes.

As follows from structural considerations, it is reasonable to assume different values of the charges *Z(k)* and radii *R(k)* for $Cs_1$ and $Cs_2$ and $Br_1$, $Br_2$ and $Br_3$ atoms. As was shown in reference [16], these are eleven Br atoms around $Cs_1$ and nine Br atoms around $Cs_2$, which leads to a much smaller valence of $Cs_1$ compared to $Cs_2$. The calculated valence sum in the phase around $Cs_1$ was 0.53 whereas that around $Cs_2$ was 1.02. A similar relation between the $Cs_1$ and $Cs_2$ effective charges for the $Cs_2CdBr_4$ crystal was obtained in the present study. The values of the effective parameters are listed in Table 3.

The numerical simulations of the lattice dynamics of $Cs_2CdBr_4$ crystal were carried out using the program DISPR [22], modified in the way as to take into account the stretching and bending interactions within the $CdBr_4^{2-}$ groups.

Frequencies calculated at the Brillouin centre mode are presented together with the experimental data in Table 1. Using an eigenvector analysis of calculated frequencies one can classify the experimental frequencies. It follows immediately from such an analysis that the last three highest-frequency modes of $A_g$ and $B_{2g}$ type and also of one of the most high-frequency mode of $B_{1g}$ and $B_{3g}$ species have a predominantly internal character. The relevant assignment of these internal stretching $\nu_1$ and $\nu_3$ vibrations is indicated in Table 1. The last but one and the last but two highest frequency modes of $B_{1g}$ (at 105 and $cm^{-1}$) and $B_{3g}$ (at 107 and 146$cm^{-1}$) symmetry also reveal a predominantly internal type. For example, the displacements of Cd and Br atoms in the sixth and the seventh modes of $B_{1g}$ and $B_{3g}$ symmetry are two orders of magnitude larger than those of first to fifth modes. Probably, these modes can be identified as $\nu_2$ and $\nu_4$ bending vibrations. It is seen from the consideration of eigenvectors that the rest of the modes of $B_{1g}$ and $B_{3g}$ types are mixed external-internal ones.

## Conclusions

The Raman spectra of the $Cs_2CdBr_4$ crystal reveal an appearance of lines forbidden by group-theory in the spectral region corresponding to the stretching vibrations of $CdBr_4^{2-}$ tetrahedron. Most probably, such a phenomenon is induced by the violation of $CdBr_4^2$ local symmetry. Two different mechanisms can evoke this effect. First, as it was suggested by Massa *et al* [18] the existence of intrinsic crystal defects can mainly influence the tetrahedron sublattice. Therefore, the local symmetry of $CdBr_4^2$ clusters appears to be lowered in respect to the demands of *Pnma* space group. Secondly, the regions of incommensurate modulation may dynamically appear far above the phase transition into the incommensurate phase [23]. It is obvious, that such a modulated structure loses the center of inversion that should be present at room temperature.

Consequently, a few new lines, which are connected with long-range disorder of the tetrahedra, can appear in Raman spectra. Note, due to the low values of bending mode frequencies the appearance of new modes in spectra of $Cs_2CdBr_4$ can be detestable only at the highest frequencies corresponding to the stretching vibrations.

The investigation of lattice stability of $Cs_2CdBr_4$ crystal reveals a non-equivalent distribution of effective charges of both $Cs_1$ and $Cs_2$

Table 3. Effective charges and radii used in atomistic model simulation of $Cs_2CdBr_4$ crystal in *Pnma* phase.

| Type of ion, k | $Cs_1$ | $Cs_2$ | Cd | $Br_1$ | $Br_2$ | $Br_3$ |
|---|---|---|---|---|---|---|
| Z(k) | 0.533 | 1.099 | 0.727 | -0.566 | -0.643 | -0.575 |
| R(k) | 2.853 | 2.808 | 0.833 | 1.506 | 1.524 | 1.546 |

and of $Br_1$, $Br_2$ and $Br_3$ ions. The large difference between the $Cs_1$ and $Cs_2$ charges amounts to a factor two (0.53 and 1.02, respectively).The reasonable agreement between the calculated and experimental values of the phonon frequencies reveals the expediency of the $Cs_2CdBr_4$ lattice dynamics simulation using and interatomic potential which includes long-range Coulombic, short-range and covalent-bond interactions. The majority of phonon modes reveal a mixed external-internal character. However, two low-frequency modes of $B_{1g}$ and $B_{3g}$ symmetry underlying in the region of lattice modes can be identified as predominantly internal (bending) vibrations of $CdBr_4^{2-}$ tetrahedra.

## References


1. Altermantt D, Arend H, Niggli A and Petter W. Mater. Res. Bull. **14**, (1979) 139.
2. Plesko S., Kind R. and Arend H. Ferroelectrics, **26**, (1980) 703.
3. Plesko S., Kind R. and Arend H. Phys. Status Solidi (a), **61**, (1980) 87.
4. Maeda M., Honda A. and Yamada N. J. Phys. Soc. Japan, **52**, (1983) 3219.
5. Altermatt D., Arend H., Gramlich V., Niggli A. and Petter W. Acta Cryst., **B40,** (1984) 347.
6. Zaretskii V. and Depmeier W. Abstract from 7th European Meeting on Ferroelectricity (Dijon: Univercity of Burgundy), (1991) 207.
7. Kityk A.V., Mokry O.M, Soprunyuk V.P. and Vlokh O.G. J.Phys.:Condens. Matter, **5**, (1993) 5189.
8. Kuzel P., Moch P., Gomez-Cuevas A. and Dvorak V. Phys. Rev. B, **49**, N10, (1994) 6553.
9. Kuzel P., Dvorak V. and Moch P. Phys. Rev. B, **49**, N10, (1994) 6563.
10. Rodriguez V., Couzi M., Gomez-Cuevas A. and Chaminade J.P. Phase Transitions, **31**, (1991) 75.
11. Torgashev I., Yuzyuk Yu. I., Burmistrova L. A., Smutny F. and Vanek P. J. Phys.: Condens. Matter, **5**, (1993) 5761.
12. Shchur Ya., Kamba S.and Petzelt J. J.Phys.:Condens. Matter, **11**, (1999) 3601.
13. Shchur Ya., Kamba S. and Petzelt J. J.Phys.:Condens. Matter, **11**, (1999) 3615.
14. Vanek P., Studuicka V. and Havrankova M. Mater.Res.Bull., **31**, №1, (1996) 113.
15. Nakamoto K. Infrared and Raman Spectra of Inorganic and Coordination Compounds, John Wiley & Sons, New York 1978.
16. Altermantt D., Arend H., Gramlich V., Niggli A. and Petter W. Acta Crystallogr. B **40**, (1984) 347.
17. Itoh K., Hinasada A., Matsunaga H.and Nakamura E. J.Phy.Soc.Jpn.,**52**, (1983) 664.
18. Massa N.E., Ullman F.G. and Hardy J.R. Phys.Rev.B, **27**, (1983) 1523.
19. Noiret I., Guinet Y. and Hedoux A. Phys.Rev.B, **52**, (1995).13206.
20. Chaplot S.L., Rao K.R. and Roy A.P. Phys. Rev. B**, 29**, (1984) 4747.
21. Kitaigorodskii A.I. and Mirskaya K.V. Kristallografiya, **9**, (1964) 174. (in Russian)
22. Chaplot S.L Rep. BARC-N972, Bhabha Atomic Research Center, Bombay, 1978.
23. de Pater C.J. Acta Crystallogr. **B 35**, (1979) 299.